

Neutron flux intercomparison and ex-core neutron detector optimization in a SMR reactor using MCNP6 code and MAVRIC sequence

Gregório Souza¹, Thiago Carluccio¹, Priscila Sanchez¹ and Alfredo Abe²

¹ Centro Tecnológico da Marinha em São Paulo –
Departamento de Engenharia de Reatores Nucleares
Av. Professor Lineu Prestes 2468
05508-000 São Paulo, SP, Brazil
gregorio.souza@marinha.mil.br

² Instituto de Pesquisas Energéticas e Nucleares (IPEN / CNEN - SP)
Av. Professor Lineu Prestes 2242
05508-000 São Paulo, SP, Brazil

ABSTRACT

Ex-core neutron detectors are commonly referred as a detector placed outside the reactor pressure vessel and in a typical SMR design its use is employed to reactor control. Due to its position (far from core) neutron flux calculation for ex-core detector purposes is challenging when using Monte Carlo codes, therefore this work presents an intercomparison between two Monte Carlo codes and also a neutron flux analysis (axially and radially) to better positioning the ex-core neutron detectors. Discrepancies regarding energy treatment can be evaluated as the MAVRIC sequence uses a set of cross sections in a multigroup energy structure while MCNP6 uses continuous energy. In this work, neutron flux intercomparison is mostly focused on variance reduction techniques since these codes presents different approaches, mainly because the MAVRIC sequence uses a hybrid approach combining deterministic and probabilistic methods and MCNP6 code uses traditional variance reduction methods. Some Monte Carlo variables such as figure-of-merit, CPU-time and error distributions maps are evaluated, and neutron flux magnitudes compared. To do so, a typical small modular reactor is modeled with the aid of MCNP6 code and the MAVRIC sequence in two different situations: one being a deep subcritical state with an external neutron source for variance reduction techniques comparison and the other a generic start up procedure (control rods removal) for detector position optimization.

1. INTRODUCTION

In the last few years several countries as Canada, UK, China, France and USA had been investing in R&D to develop the concept of a small modular reactor (SMR) [1]. These kind of reactors would have some advantages when compared with the common ones: it could be fabricated at a plant and mounted on site by coupling several modules depending on the total power required. Moreover, the standardized SMR design could facilitate the project licensing process remaining, as major challenge, the construction site authorization by the competent government agency. It could improve general costs consequently reducing energy price to final consumers due to shortening the path until startup. This work presents its results based on a typical SMR of low enriched uranium UO₂ fuel rod type containing 21 fuel assemblies. These assemblies are arranged as a 17x17 matrix in a regular PWR pitch size and the fuel active length in the core is around 1 meter. Reactor power control is realized by B4C or Ag-In-Cd banks while the safety function is performed by additional banks.

Reactor core configuration and details is not paramount as this works is focused on flux comparison in regions outside the reactor pressure vessel between MCNP6[2] and MAVRIC[3] both Monte Carlo codes. All comparisons are made considering identical

materials, geometry and modelling with the same ENDF/B-VII.1 data library[4]. Different variance reduction techniques are utilized in the MCNP6 and MAVRIC and their results are compared with each other to better understand these techniques and to judge which one is ideal to a hypothetical reactor start up procedure in an ex-core neutron detector positioning optimization.

2. METHODOLOGY

2.1. Variance Reduction in Monte Carlo Transport Codes MCNP6 and MAVRIC

The difficulty of using Monte Carlo techniques is to minimize the computing time necessary to achieve a tally estimate with a good relative error and to also achieve positives results on all the statistical tests [5] that is necessary to affirm that the simulation is trustworthy. Basically, the simulation is modified in such way that the result produces few or non zero-score tallies and this is important mainly for deep penetrations shielding problems. There are several ways to change the simulation, but they can be divided in three major groups. The first one is to use truncation methods where the particle history is terminated following user defined criteria, the second one is to use the particle importance (in energy, space or time) to control the overall population and the third one is to use partially deterministic methods. Clearly, the Monte Carlo users desire to achieve a relative error with the smallest number of histories and generally relative errors should be less than 5% to produce meaningful results. On Monte Carlo codes increasing the number of histories is a poor way of reducing the relative error and every Monte Carlo has its own set of options and capabilities in variance reduction techniques.

In this work the MCNP6 is utilized with two different variance reduction techniques, the first one is the weight window generator option that produces region importances in a automatic form and the second one is the use of manually inputted cell importances. For comparison purposes MAVRIC is also utilized with two different variance reduction calculations as the only variance reduction technique available is to use the deterministic DENOVO[6] code for region importance determination.

2.2. Problem Characterization – Geometry and Materials

The small modular pressurized water reactor proposed in this work is a simple 21 fuel assembly each one containing low enrichment UO₂ fuel and control rods (Ag/In/Cd or B4C) distributed evenly and symmetrically in a 17x17 matrix. The active length is around 1meter and the outer core geometry is consisted of cylindrical shells representing radially (from inner sense to outer direction) the core thermal shield (barrel), pressure vessel steel, pressure vessel thermal insulation and two steel layers with air inside representing the ex-core detector placement region. Figure 1 presents a schematic view of the modeled geometry and table 1 presents all the geometry dimensions.

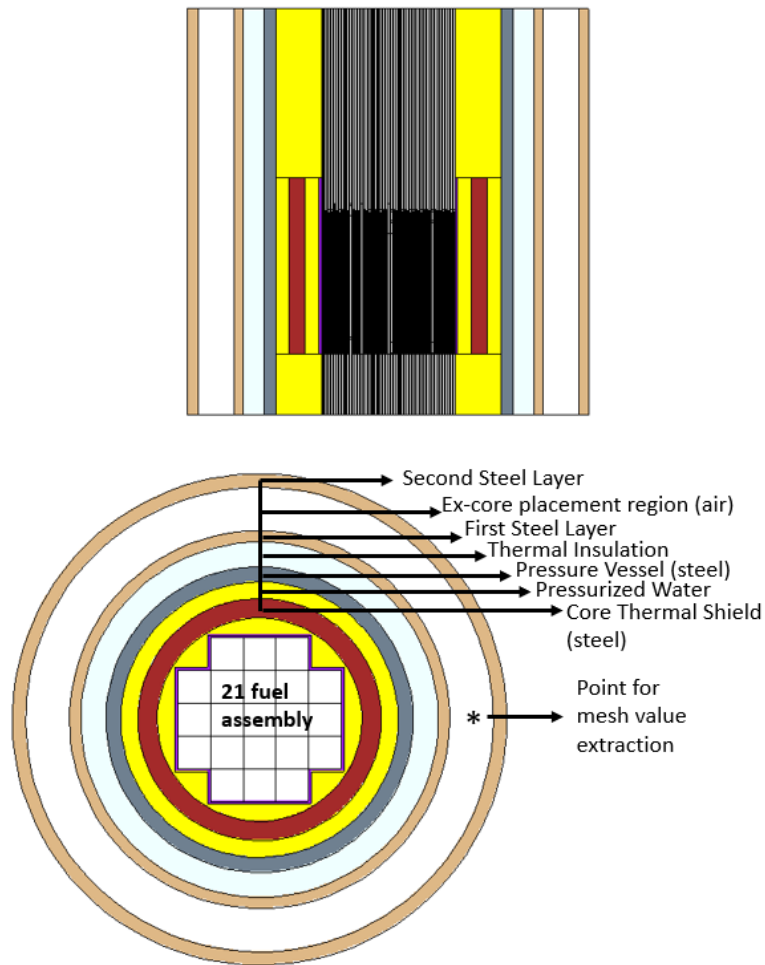


Figure 1: Schematic view of the modeled geometry (MCNP6 VisEd Plot).

Table 1: Outer Core Geometry Dimensions

Geometry Component	Thickness (cm)	Length (cm)	Density (g/cm ³)
Core Thermal Shield (barrel)	13	124.5	7.6
Pressure Vessel	10	335.6	7.6
Thermal Insulation (mix steel + air)	16.75	335.6	0.1
First Steel Layer	7.6	335.6	7.7
Ex-core detector placement region	29.15	335.6	0.001

The pressurized water inside the pressure vessel cylindrical shell has a density of 0.76 g/cm³.

3. RESULTS

3.1. Variance Reduction Analysis

For the purpose of the variance reduction analysis 4 source points emitting isotropic neutrons at the 3 MeV energy are simulated inside the core thermal shield and near the reactor core. All control banks are fully inserted. Figure 2 presents the 4 source points location in the geometry model. Table 2 presents a short description for each of the cases for both MCNP6 and MAVRIC simulations.

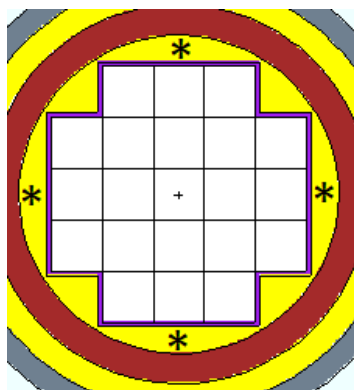


Figure 2: Source Points locations

Table 2: Short Description of the MCNP6 and MAVRIC cases

Case Identification	MCNP6	MAVRIC
0	Analog	Analog
1	Weight Window Generator (WWG)	Coarse Mesh for Sn calculation
2	Manually inputted importances	Fine Mesh for Sn Calculation

The mesh size that encompass all the geometry for both codes consists of a rectangular mesh of $5 \times 5 \times 5 \text{ cm}^3$ cell dimension. Was requested for both codes to compute only the total neutron flux and all simulations were performed using a Intel Core i7-8700, 8GB, 1TB, Windows 7 Hewlett Packard desktop computer. The total number of 20 million histories per case were kept fixed for both codes.

3.1.1 MCNP6 code Results

For the MCNP6 Weight Window Generator (WWG) simulation (case 1) the following setup was chosen: reference calculation is a F4 tally type at the ex-core detector placement region, the WWG is an energy weight window type with the core thermal shield (barrel) having 50% of the source weight. The other MCNP6 simulation is the one that the importances were inputted manually (case 2), these importances increased radially 4 times at each cell crossing

starting at the source area (inside the core thermal shield) with importance equal to one. Figures 3 to 5 presents the MCNP6 results for the case 0, 1 and 2 respectively.

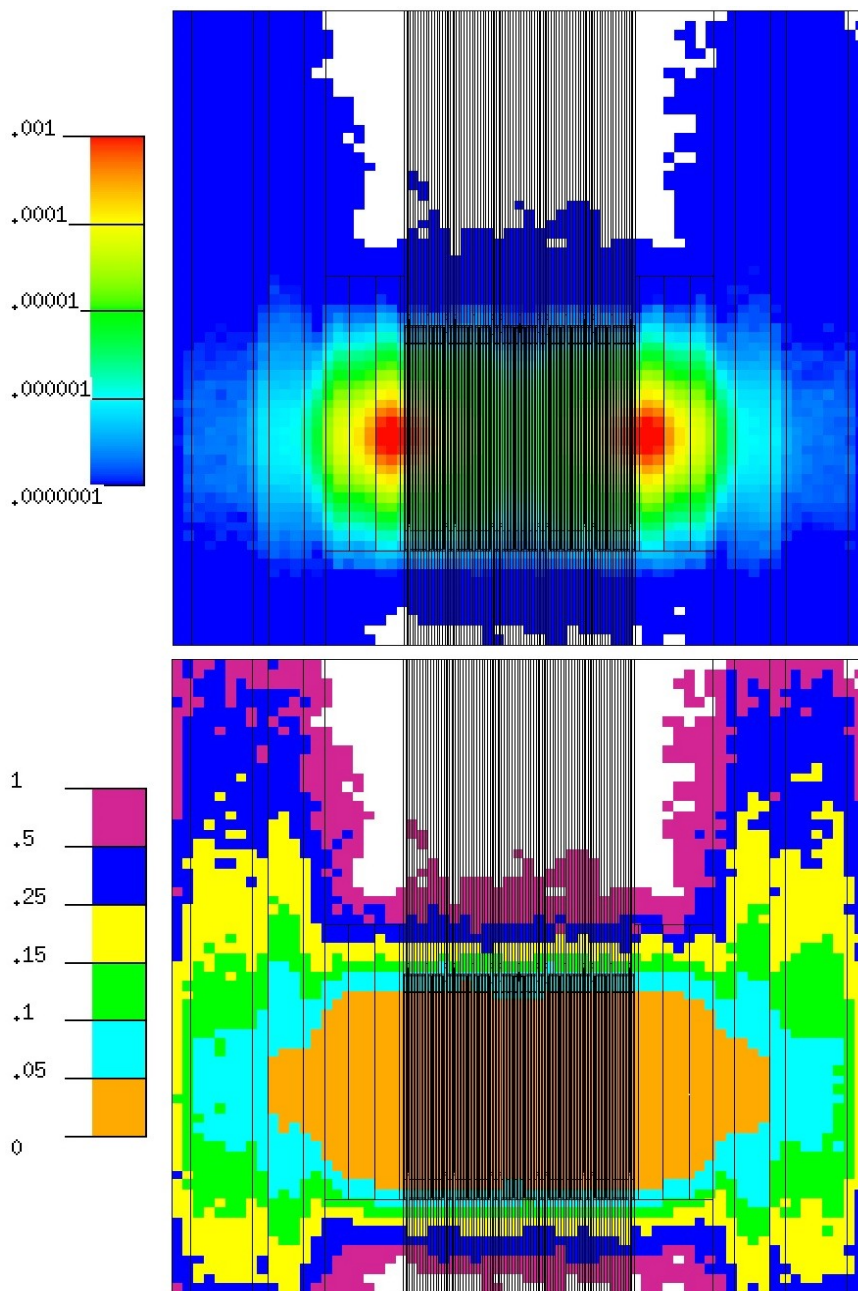


Figure 3: MCNP6 Results for the total neutron flux distribution for the case 0 – Analog Simulation - [cm⁻² · source particle⁻¹]. Relative error distribution at the bottom.

Figure 3 above presents the analog case and the behavior is as expected. The converged area (relative error inferior to 5%) is only around the source region and the relative error increases with source distance. Case 0 has zero-score tallies above the core region which is natural as this region is fulfilled with the pressurized water (typical high attenuation profile for neutrons).

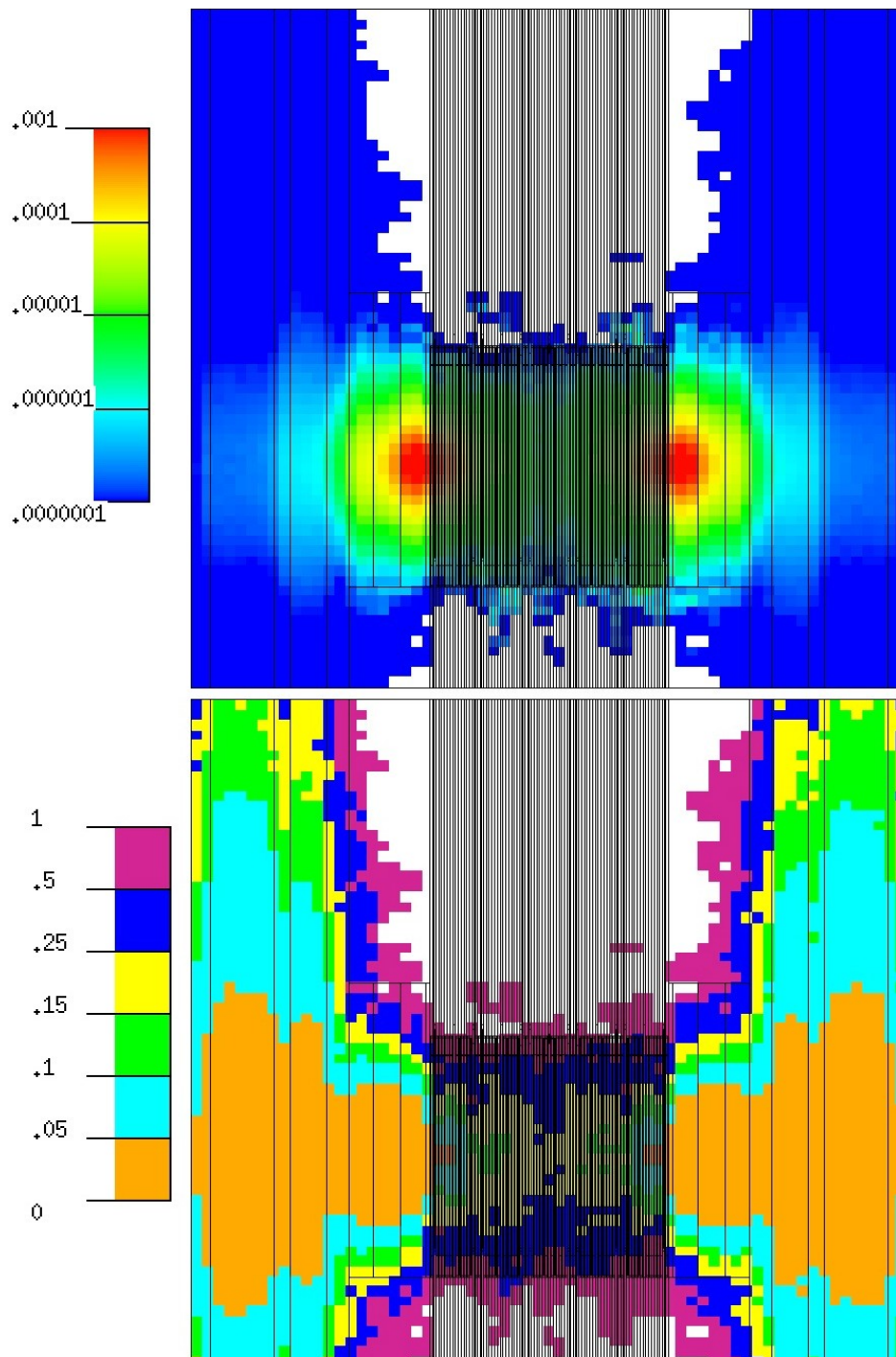


Figure 4: MCNP6 Results for the total neutron flux distribution for the case 1 – Weight Window Generator (WWG) Simulation - [$\text{cm}^{-2} \cdot \text{source particle}^{-1}$]. Relative error distribution at the bottom.

Figure 4 above presents the WWG case and the results are more converged, and the total neutron flux is smoother than the case 0. The neutron flux is pushed through the source area to the ex-core detector position by means of the weight windows. This effect is noticeable on the error distribution (right side of figure 4). Case 1 has also zero-score tallies above the core region which is natural as this region is fulfilled with the pressurized water (typical high attenuation profile for neutrons).

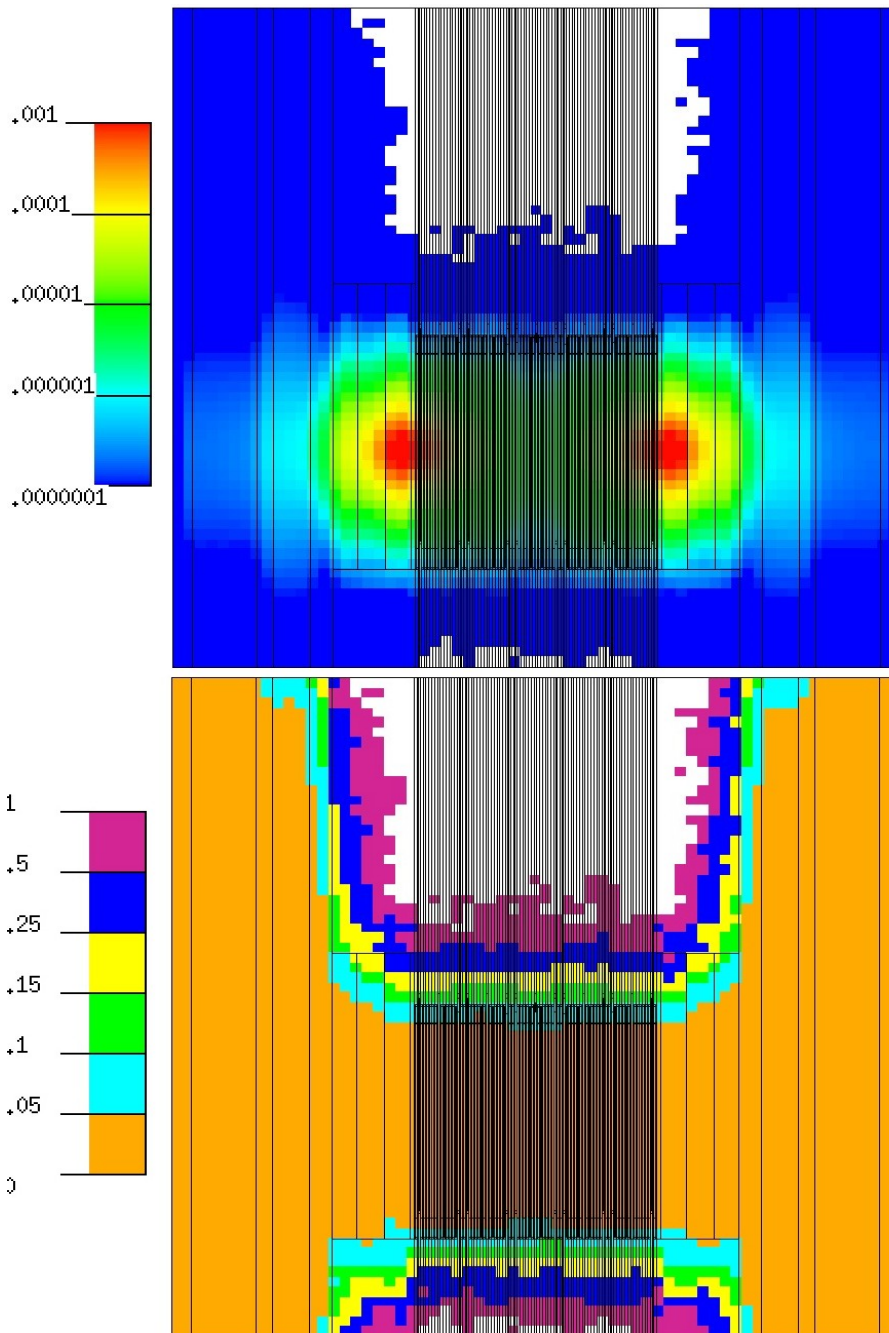


Figure 5: MCNP6 Results for the total neutron flux distribution for the case 2 – Importances Inputted Manually Simulation - [$\text{cm}^{-2} \cdot \text{source particle}^{-1}$]. Relative error distribution at the bottom.

Figure 5 above presents the results from the importances that were inputted manually on the cells and as it can be seen in the converged area (areas with relative error less than 5%) the particles are pushed through the splitting game of the reduction variance technique in all the cell extension (bottom to top) that received the importances manually (cylindrical shell representing the pressure vessel, thermal insulation and steel layers). Case 2 has also zero-score tallies for the region above the core which indicates that several splits were made radially and not axially and that is in total agreement with the importances that were inputted manually as they were increased by factor of 4 in each cylindrical shell.

3.1.2 MAVRIC Results

The MAVRIC code is actually a sequence of codes for shielding applications. The DENOVO code a Sn (Discrete Ordinates Method) deterministic solver provides MONACO importance calculations in a rectangular mesh that overlays all the geometry. This procedure is automatic therefore the MAVRIC acronym (**M**onaco with **A**utomated **V**ariance **R**eduction using **I**mportance **C**alculations). The user is left to choose some parameters to control the Sn solver but the most important is the choice for the mesh dimension. The MAVRIC results for this work come from two different meshes. One is a coarse mesh (case 1) with 10 x 10 x10 cm dimensions and the other is a fine mesh (case 2) with 2.5 x 2.5 x 2.5 cm dimensions. Figures 6 to 8 presents the MAVRIC results for the case 0, 1 and 2 respectively.

Figure 6 presents the analog case and the behavior is as expected. The converged area (relative error inferior to 5%) is only around the source region and the relative error increases with source distance. The overall behavior is like the case 0 for the MCNP code (see figure 3).

Figure 7 above presents the coarse mesh case results and the total neutron flux is computed in all the geometry. There are no zero-score tallies in any region of the model. The neutron flux is pushed through everywhere by means of the importance calculations made on the Sn stage. The region above the core has relative error up to 15% and in other regions the relative error is very well converged and up to 5%.

Figure 8 above presents the fine mesh case results and the total neutron flux is also computed in all the geometry. Also, as in the case 1 there is no zero-score tallies in any region of the model. The neutron flux is pushed through everywhere by means of the importance calculations made on the Sn stage and the region above the core has relative error up to 5% and in other regions the relative error is extremely well converged and up to 3%.

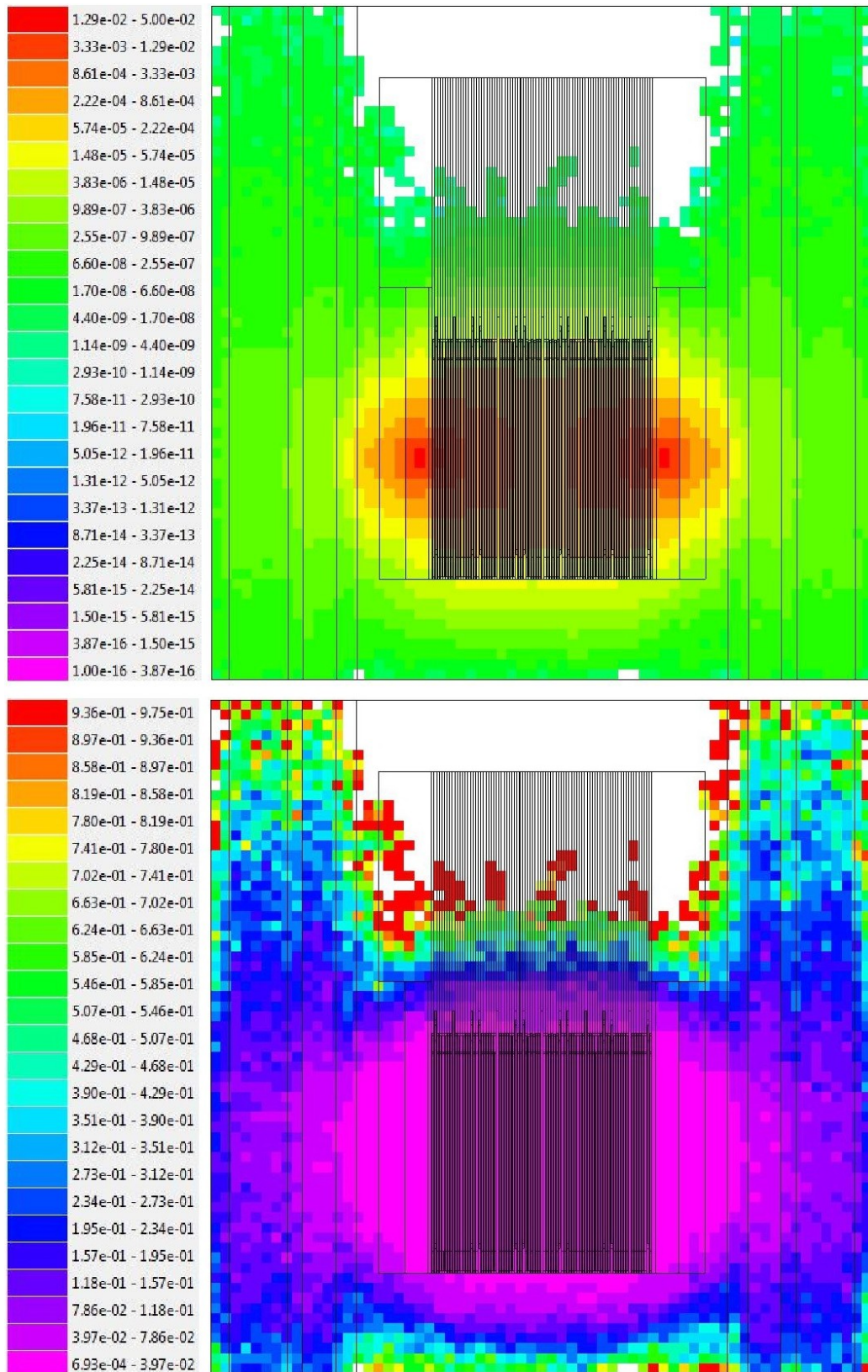


Figure 6: MAVRIC Results for the total neutron flux distribution for the case 0 – Analog Simulation - [$\text{cm}^{-2} \cdot \text{source particle}^{-1}$]. Relative error distribution at the bottom.

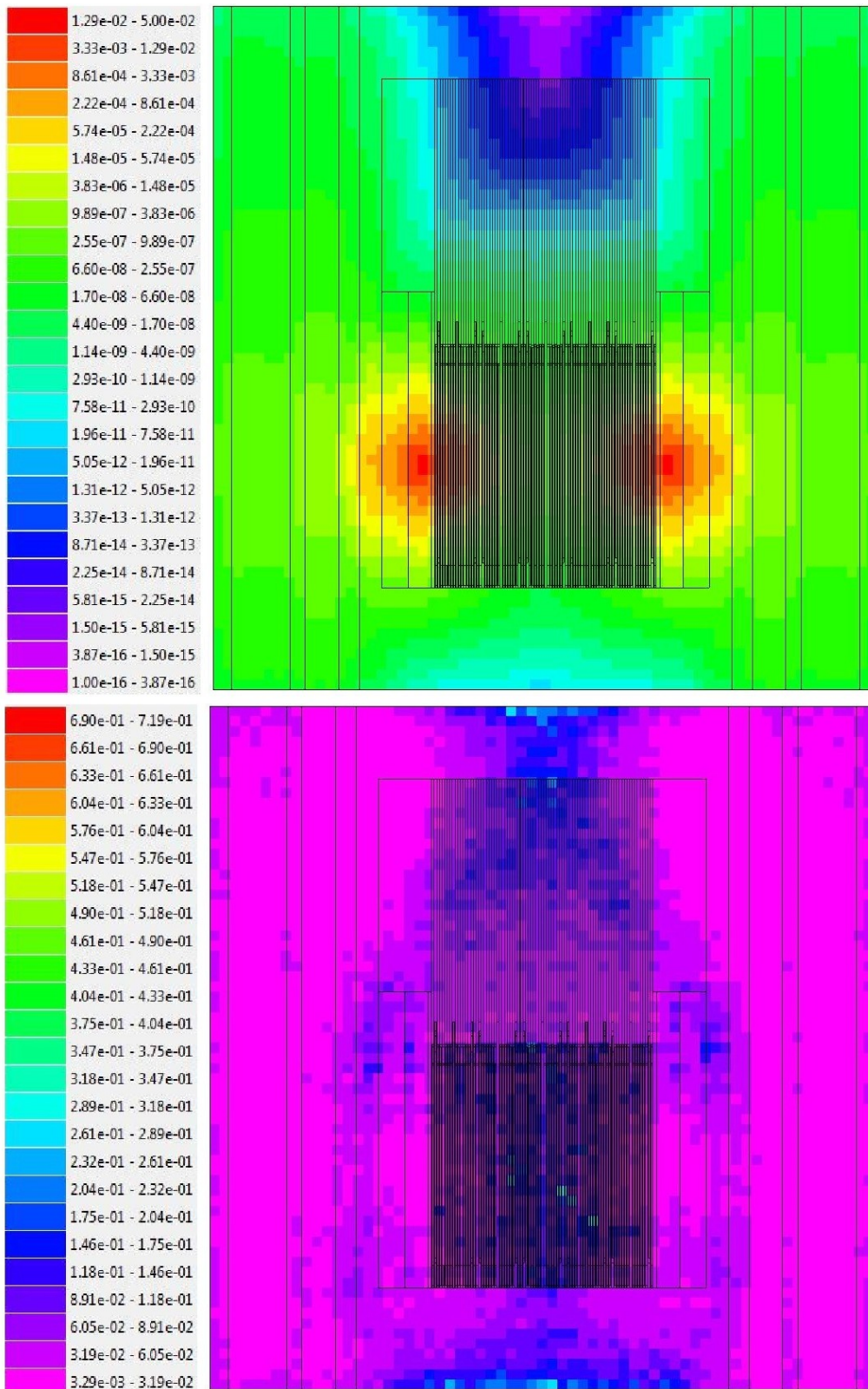


Figure 7: MAVRIC Results for the total neutron flux distribution for the case 1 – Coarse Mesh for the Sn Importance Calculation - [$\text{cm}^{-2} \cdot \text{source particle}^{-1}$]. Relative error distribution at the bottom.

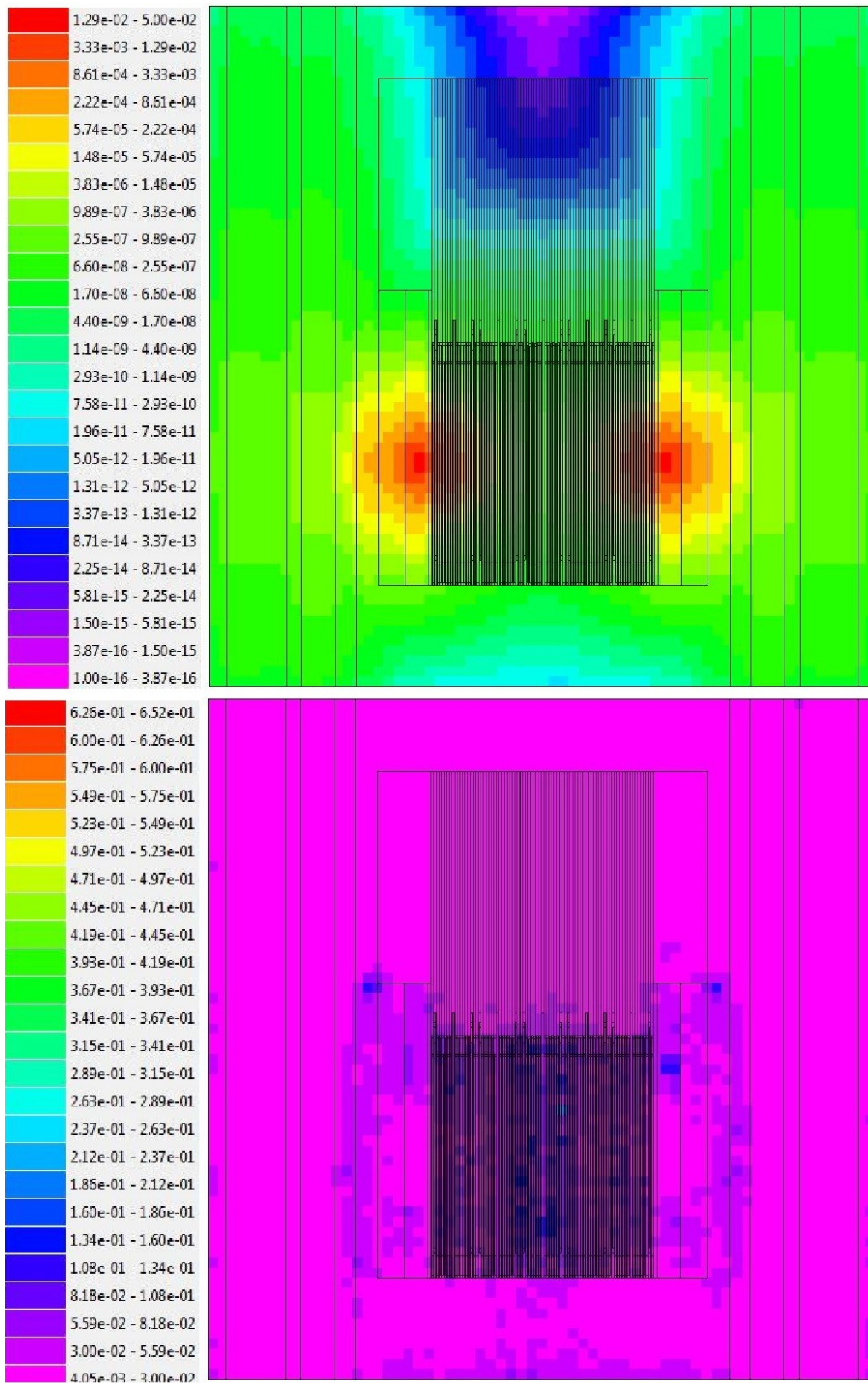


Figure 8: MAVRIC Results for the total neutron flux distribution for the case 1 – Fine Mesh for the Sn Importance Calculation - [$\text{cm}^{-2} \cdot \text{source particle}^{-1}$]. Relative error distribution at the bottom.

3.1.3 MCNP6 x MONACO – Flux Comparison and Variance Reduction Analysis

Using the location adopted for the mesh value extraction (see figure 1) the results for total neutron flux are presented on table 3 along with each simulation Figure of Merit (FOM) for both codes.

Table 3: Neutron Flux Comparison and Figures of Merits (FOMs)

	MCNP 6			MAVRIC sequence		
	Case 0	Case 1	Case 2	Case 0	Case 1	Case 2
Total Neutron Flux (cm ⁻² .source particle ⁻¹)	1.48E-07	1.61E-07	1.57E-07	5.27E-07	4.54E-07	4.55E-07
Relative Error	1.04E-01	3.05E-02	4.45E-03	1.02E-01	1.20E-02	1.00E-02
Computer Time (minutes)	1773.7	183.7	6789.4	421.8	347.4	1752
Figure of Merit (FOM)	5.19E-02	5.86E+00	7.42E+00	2.28E-01	2.00E+01	5.71E+00

The total neutron flux computed in the MAVRIC sequence is higher than those computed on MCNP6, this difference can only be attributed to the energy treatment on the cross-section and transport calculation. The MAVRIC is a multi-group transport code and the cross section utilized is grouped in 27 groups, in this manner the 3 MeV neutron energy from the source points cannot be simulated monoenergetic as MCNP6 does. In fact, the energy group utilized in MAVRIC is around 3 to 6 MeV, keeping that in mind is reasonable to affirm that both results from MCNP6 and MAVRIC are in good agreement.

Regarding the variance reduction analysis in MCNP6, the Weight Window Generator (case 1) is the best technique applied for this work problem. The total computer time is shorter for case 1 and the results are well converged in the area of interest. As expected and warned in the MCNP6 manual even the most experienced user cannot predict the importances for all regions correctly which can be proven analyzing the results of case 2.

Finally, the MAVRIC sequence brings the game of variance reduction to another level with its automated importance calculations by means of Sn transport calculations. Obviously, the analog case for MAVRIC is similar to the analog case for MCNP6 but starting from case 1 the automated variance reduction using the CADIS methodology [7] in MAVRIC can eliminate zero-score tallies everywhere and that is most desirable matter in shielding and ex-core calculations. However, MAVRIC results from case 1 using the coarse mesh is enough and with the fine mesh MAVRIC computes practically the same result from case 1 (coarse mesh) but with almost the triple of the time. This work confirms that the Sn stage in MAVRIC can be utilized with coarser meshes when compared with the meshes constructed in an usual Sn transport calculation. The main difference in MAVRIC is that the forward flux computed in the Sn stage could be not so accurate since it serves only as hint of the real flux to construct the importance map that will be used in the second stage by MONACO on the MAVRIC sequence.

3.2. Start Up Procedure – Ex- Core Neutron Detector Positioning Optimization

A start up procedure for the small modular pressurized water reactor modeled for this work is simulated only for illustrating the viability of using a trustworthy variance reduction method. The start up procedure proposed consists of removing the control/absorber rods in 0, 16, 33 and 66 % of the fuel active length. The MCNP6 code with the variance reduction utilized in case 1 (Weight Window Generator) was chosen because it proved to be the fastest one to achieve good results in the ex-core detector region. That was the one and only prerequisite.

Through figures 9 to 12 the expected flux behavior when control/absorber rods are lifted from the core can be observed, that is the reactor buckling assuming a cosine shape as the control rods are removed. One could obviously suggest that there is no need for detector positioning optimization because if the cosine shape is observed one would always easily identify the maximum detector position. In a simple situation this is may be true but in real applications the neutron flux seems to be quite low and very sensitive neutron detectors are needed, therefore an accurate flux distribution map in the ex-core detector region may be very useful for the ones responsible for the reactor start up procedure. For the model proposed in this work the neutron flux radial profile has no edges and is very evenly distributed as it can be seen in figure 13.

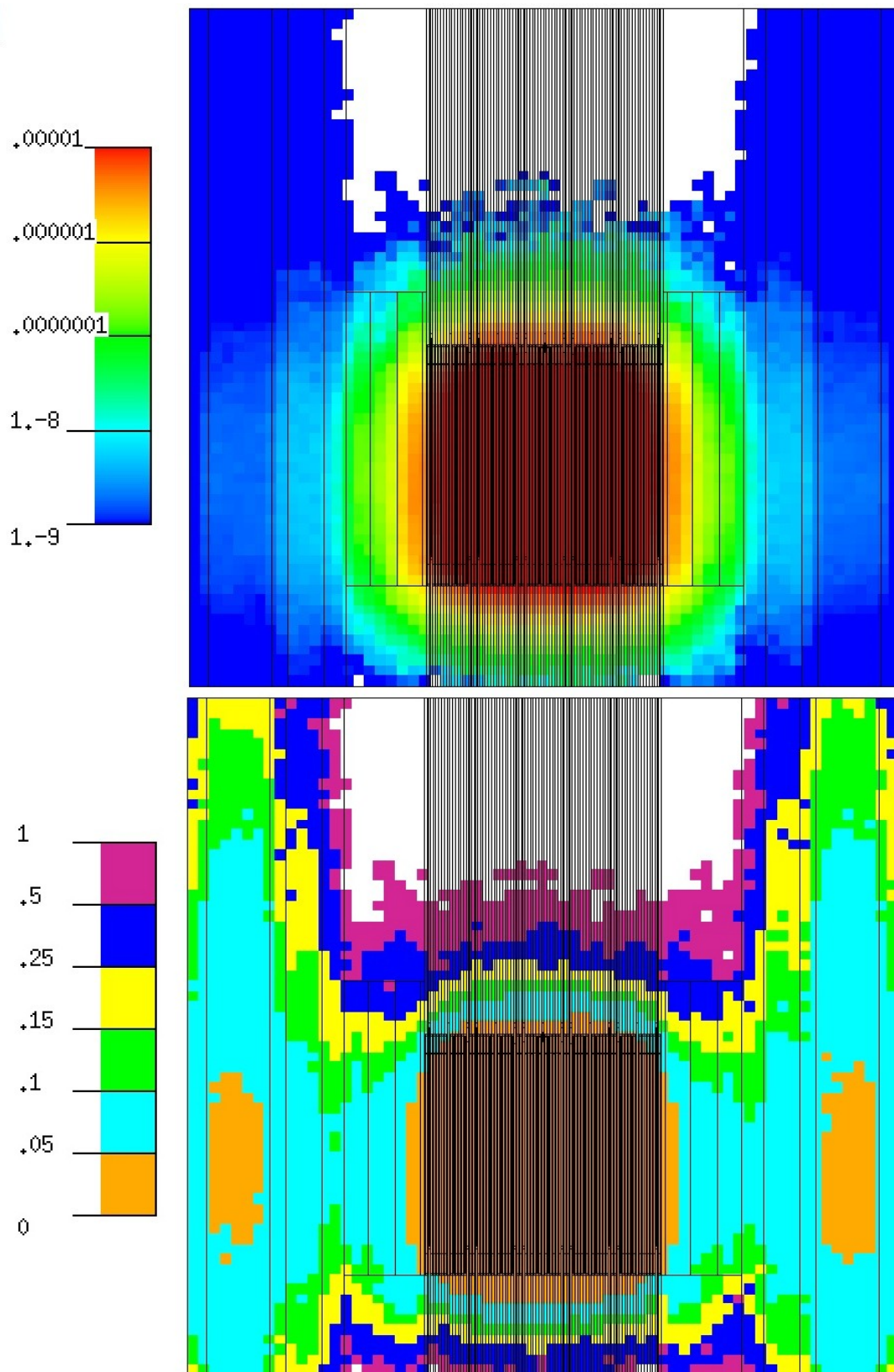


**Figure 9: MCNP6 Results for the 0% control rod removal- [$\text{cm}^{-2} \cdot \text{source particle}^{-1}$].
Relative error distribution at the bottom.**

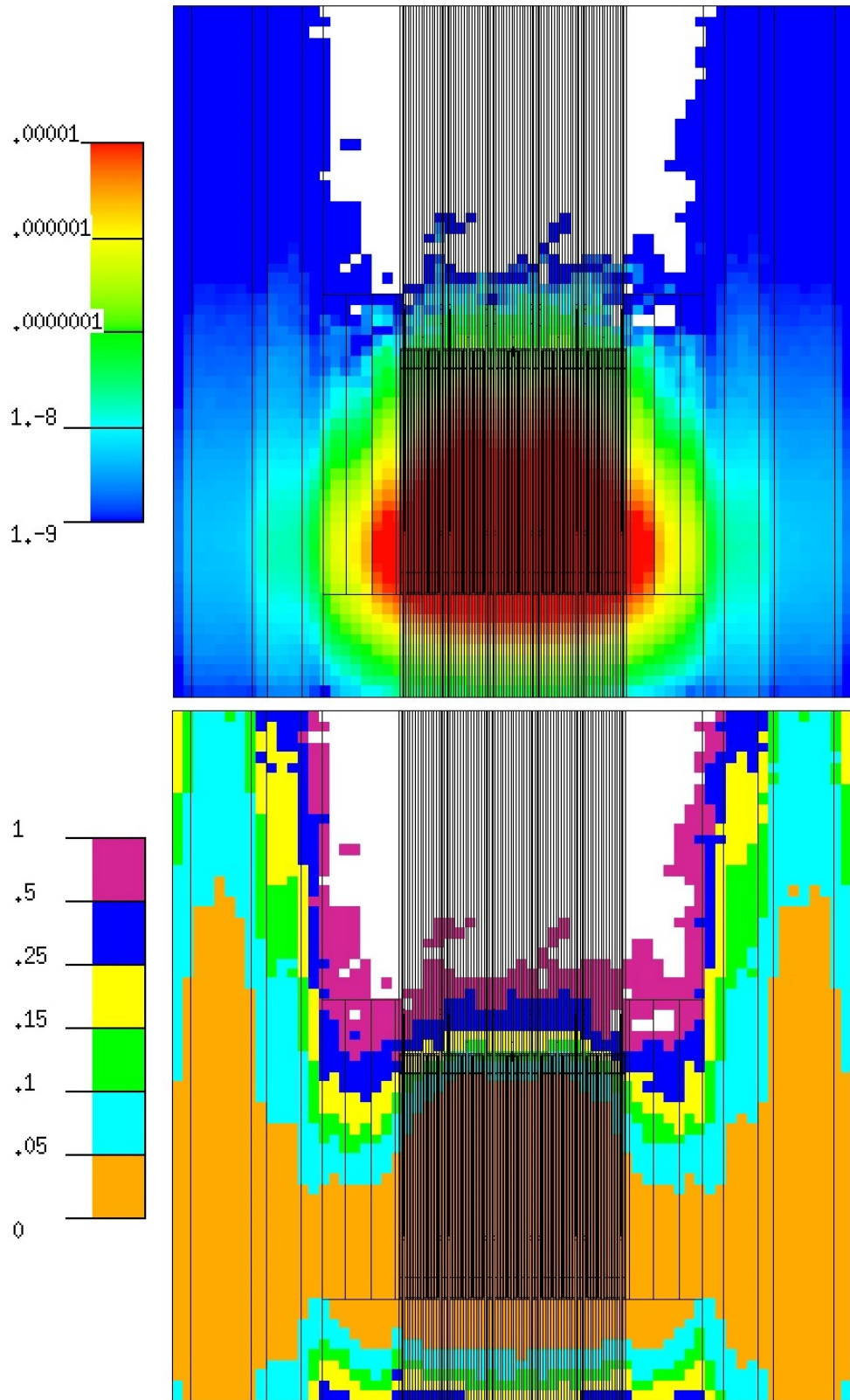


**Figure 10: MCNP6 Results for the 16% control rod removal- [$\text{cm}^{-2} \cdot \text{source particle}^{-1}$].
Relative error distribution at the bottom.**

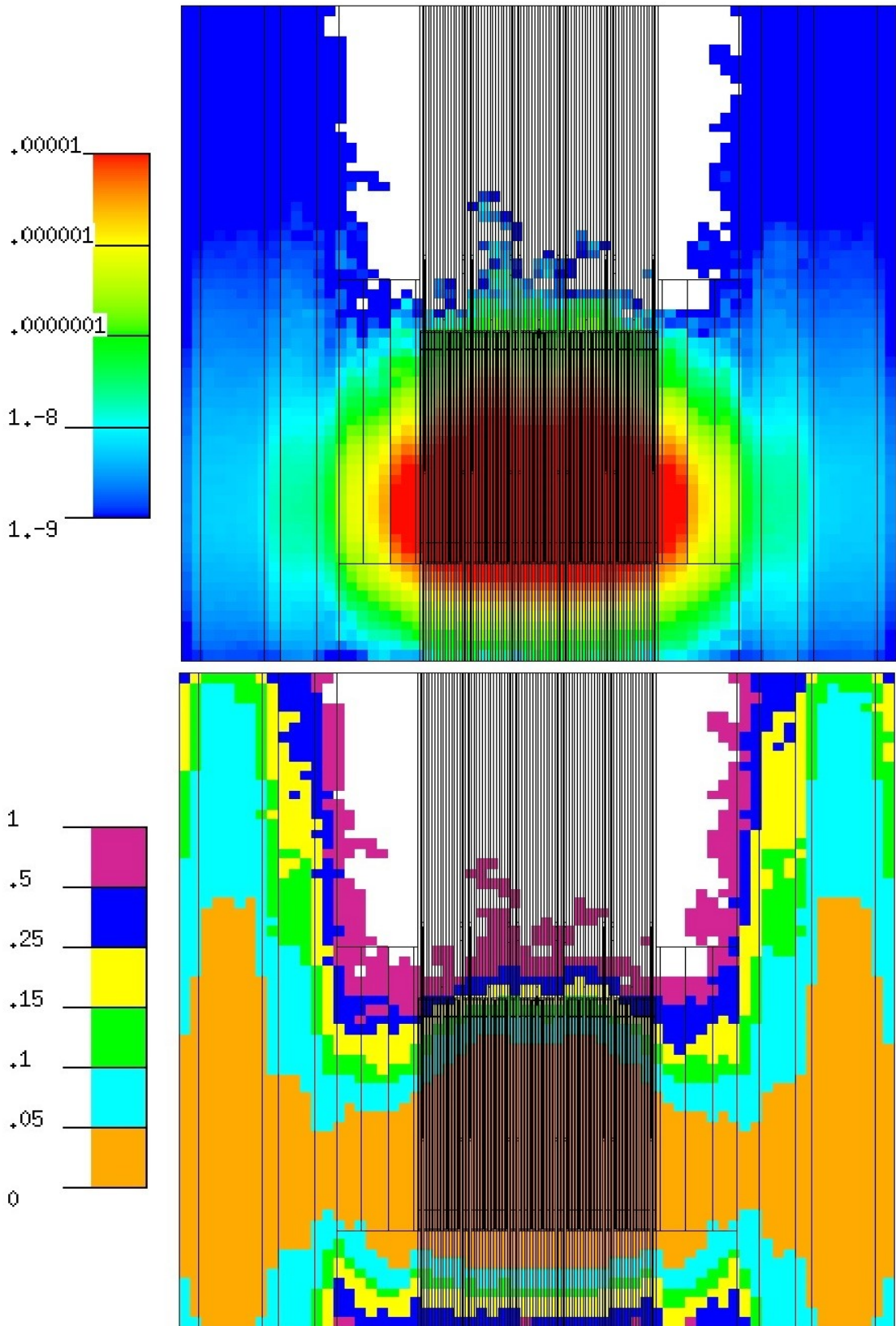


**Figure 11: MCNP6 Results for the 33% control rod removal- [$\text{cm}^{-2} \cdot \text{source particle}^{-1}$].
Relative error distribution at the bottom.**

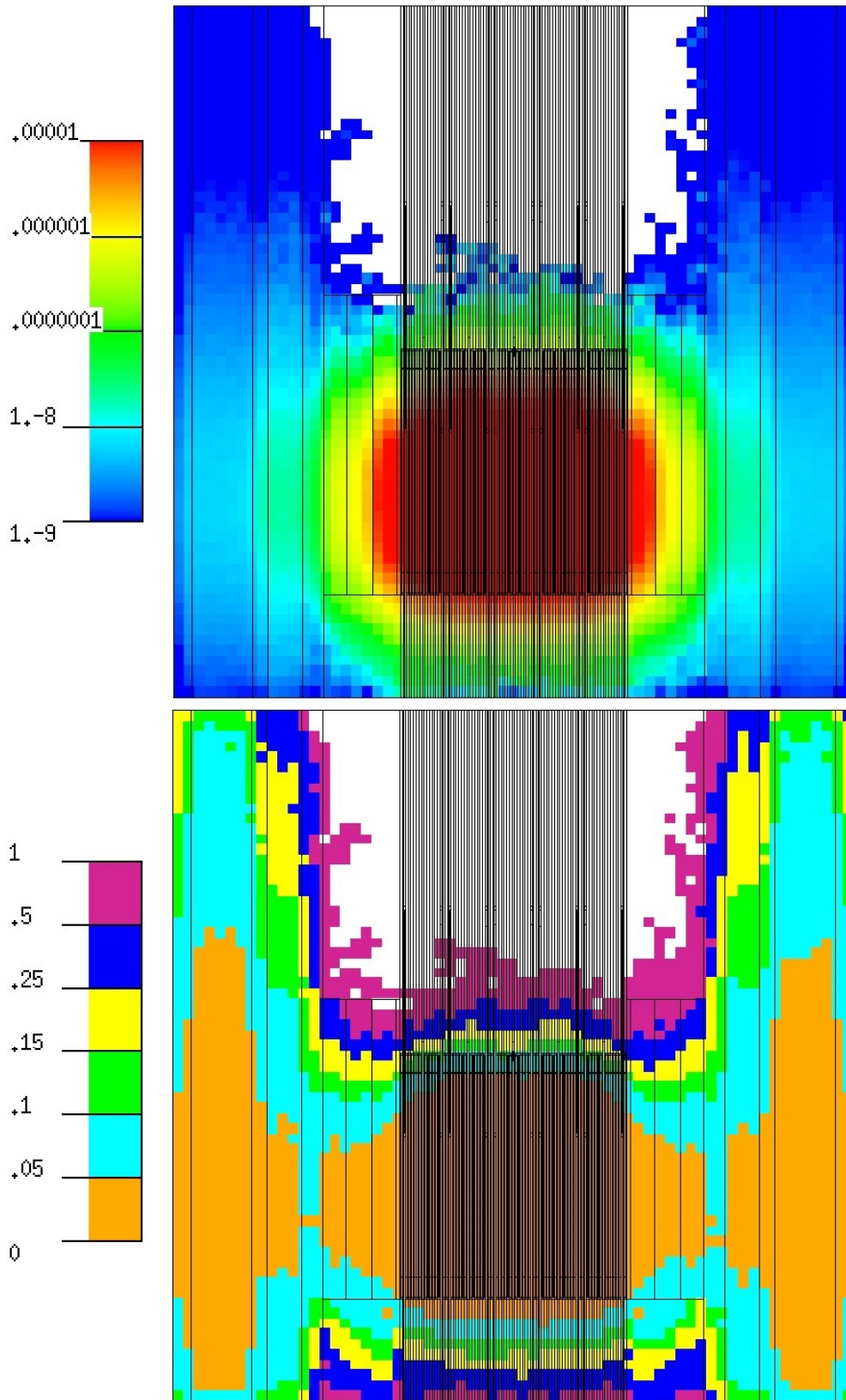


**Figure 12: MCNP6 Results for the 66% control rod removal- [$\text{cm}^{-2} \cdot \text{source particle}^{-1}$].
Relative error distribution at the bottom.**

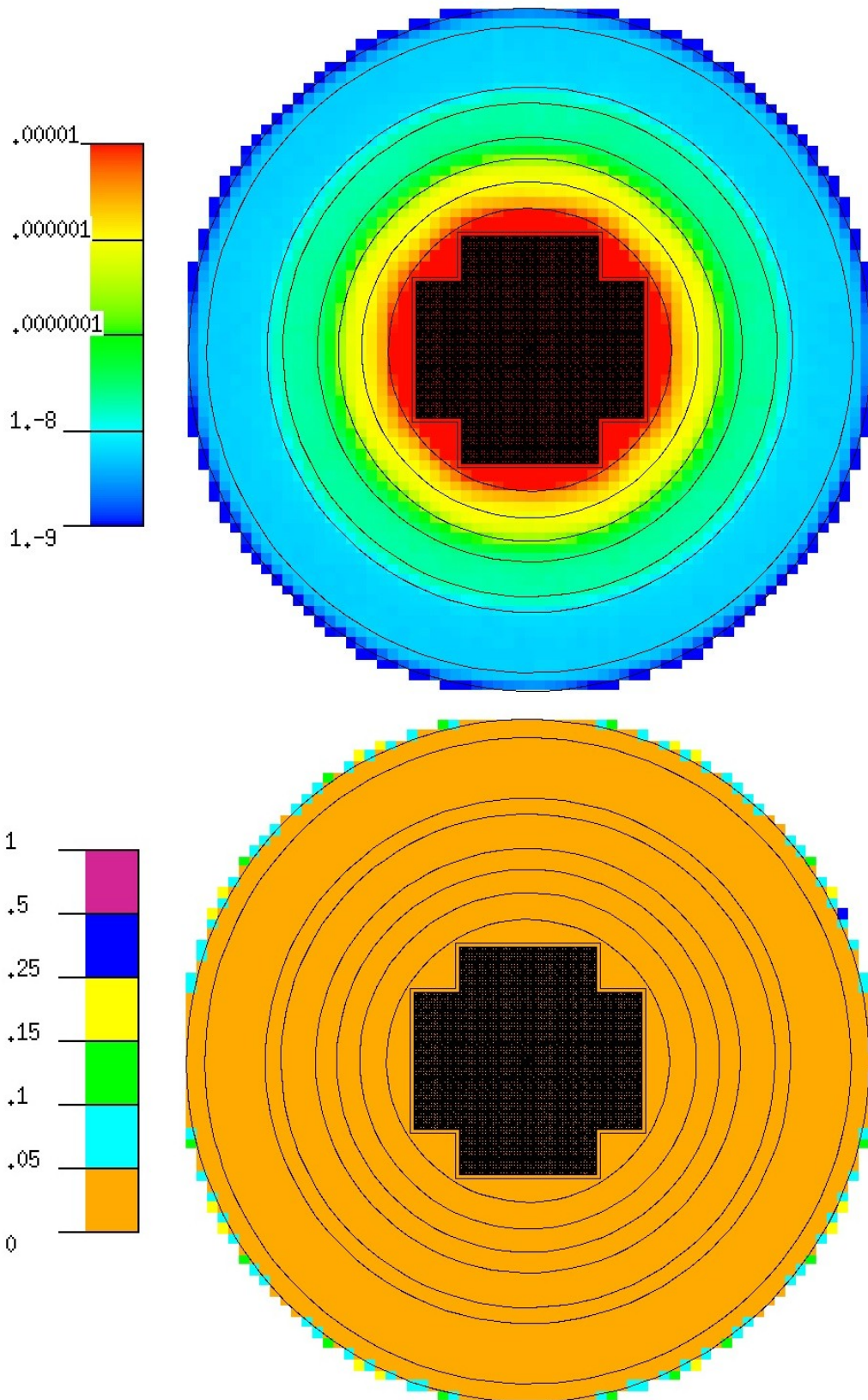


Figure 13: MCNP6 Results for the 33% control rod removal- Radial neutron flux distribution- [$\text{cm}^{-2} \cdot \text{source particle}^{-1}$]. Relative error distribution at the bottom.

In this way the only optimization process in the ex-core detector position is to seek for the optimum axial position in the ex-core detector region. As the control rod is lifted the neutron flux rises and new cosine shapes appears in the ex-core detector region. In a practical situation the detector is placed in the middle of different regions such as a start-up region (low power) and a power region where the reactor reaches more than 5% of its nominal power per example. Figure 14 presents the best position to locate an ex-core neutron detector in a start-up procedure, the range of the results are set in a way that favors the ex-core neutron detector area.

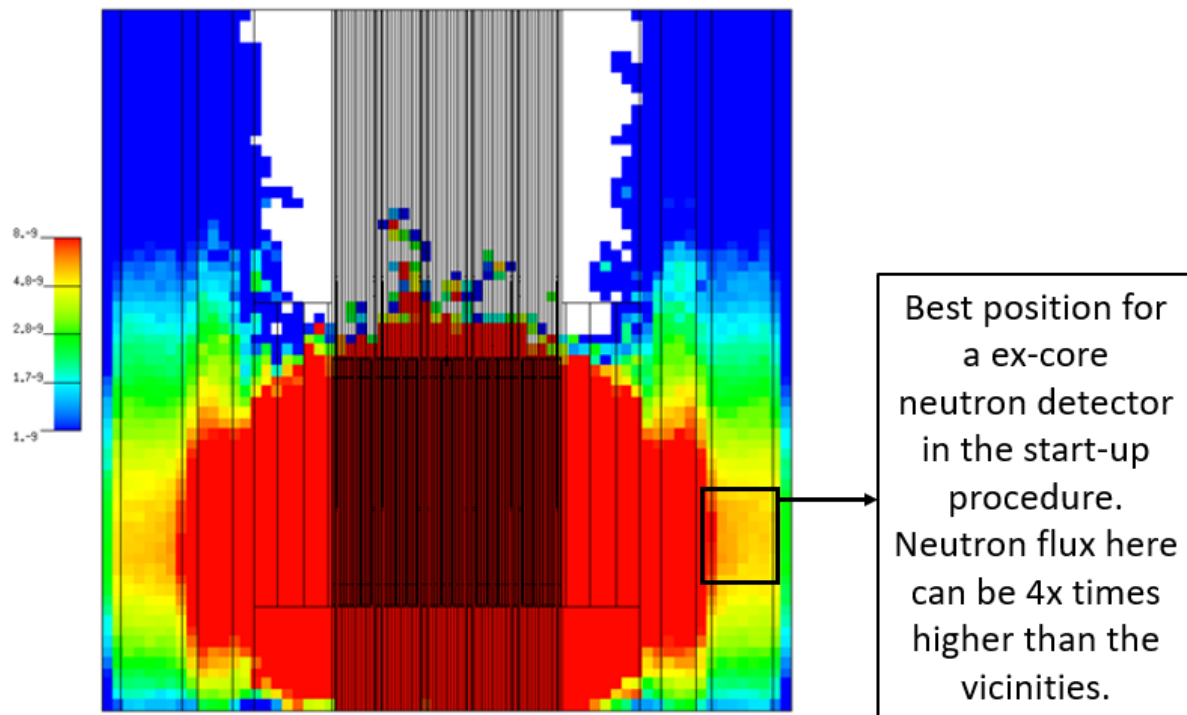


Figure 14: MCNP6 Results for the 33% control rod removal – Range set to favor the values inside the ex-core detector region- [$\text{cm}^{-2} \cdot \text{source particle}^{-1}$].

The flux profile adopted for the position chosen in figure 14 is the one from the 33% control rod removal step. Assuming that beyond this step the reactor begins to gain significant power the best position for the ex-core detector in the star-up procedure is around 20% of the active length of the fuel rod.

4. CONCLUSIONS

This works presents a useful neutron flux comparison in a typical small modular pressurized water reactor that is focused on different variance reduction techniques for the main Monte Carlo codes used for shielding and ex-core neutron calculations. Results from both codes are in the same magnitude order and considering that there is a multi-group simplification in the MAVRIC sequence the results are in good agreement. The MCNP6 presented the fastest simulation (best FOM) that can achieve good results in the ex-core detector area but all of the MCNP6 cases presented zero score tallies in challenging areas where the neutron attenuation

is severe. Contrary to these results the MAVRIC sequence did not present any zero score tallies (except for the analog case) and the error distribution maps are significant more converged. This takes away the user's responsibility to choose the best technique available for the application in mind as the MAVRIC sequence is hybrid code that uses a deterministic method to set importances everywhere in a user defined mesh. Finally, a hypothetical start-up procedure was simulated using MCNP6 and the best position for a neutron detector was elected around 20% of the active fuel length.

ACKNOWLEDGMENTS

The authors would like to thank the Navy Technological Center in São Paulo (CTMSP) and the Brazilian public company AMAZUL.

REFERENCES

1. Locatelli, G.; Bingham, C.; Mancini, M.; Small Modular Reactors: A comprehensive overview of their economics and strategic aspects. *Progress in Nuclear Energy* 73:75-85 · May 2014
2. Goorley, et al., "Initial MCNP6 Release Overview", *Nuclear Technology*, 180 , pp 298-315 (December 2012).
3. Peplow Douglas, E.; Monte Carlo Shielding Analysis Capabilities with MAVRIC; Article in *Nuclear technology* 174(2):289-313 · May 2011;
4. Kahler, A.C.; ENDF/B-VII.1 Neutron Cross Section Data Testing with Critical Assembly Benchmarks and Reactor Experiments; *Nuclear Data Sheets*, Volume 112, Issue 12, December 2011, Pages 2997-3036.
5. Haghghat, A.; Monte Carlo methods for particle transport; CRC press SBN-13: 978-1466592537.
6. Evans, T. M.; Denovo-A New Parallel Discrete Transport Code for Radiation Shielding Applications; *Journal: Nuclear Technology* Volume 171, 2010.
7. Wagner, J. C.; Peplow Douglas, E; Mosher, S. W.; FW-CADIS Method for Global and Regional Variance Reduction of Monte Carlo Radiation Transport Calculations; *Nuclear Science and Engineering*; Volume 176, 2014